Highlights of Spanish Astrophysics VI, Proceedings of the IX Scientific Meeting of the Spanish Astronomical Society held on September 13 - 17, 2010, in Madrid, Spain. M. R. Zapatero Osorio et al. (eds.)

The GaLAxy Cluster Evolution survey (GLACE): introduction and first results

M. Sánchez-Portal[1,2], J. Cepa[3,4], I. Pintos-Castro[4,3], R. Pérez-Martínez[1,2], I. Smail[5], E. Alfaro[6], B. Altieri[1], A. Aragón-Salamanca[7], C. Balkowski[8], M. Balogh[9], A. Biviano[10], A. Bongiovanni[4,3], M. Bremer[11], F. Castander[12], H. Castañeda[13], N. Castro-Rodríguez[4,3], D. Coia[1], P. A. Duc[14], J. Geach[5], I. González-Serrano[15], C. Haines[16], B. McBreen[17], L. Metcalfe[1], I. Pérez-Fournón[4,3], A. Pérez García[4,3], B. Poggianti[18], J. M. Rodríguez-Espinosa[4,3], G. P. Smith[16], G. Temporin[14], and I. Valtchanov[1]

[1] European Space Astronomy Centre (ESAC)/ESA, Madrid, Spain
[2] Ingeniería y Servicios Aeroespaciales, Madrid, Spain
[3] Universidad de La Laguna, Tenerife, Spain
[4] Instituto de Astrofísica de Canarias, La Laguna, Tenerife, Spain
[5] Institute for Computational Cosmology, Durham University, U.K.
[6] Instituto de Astrofísica de Andalucía, CSIC, Granada, Spain
[7] School of Physics and Astronomy, University of Nottingham, U.K.
[8] GEPI, Observatoire de Paris & CNRS, Meudon, France
[9] Department of Physics and Astronomy, University of Waterloo, Canada
[10] INAF, Osservatorio Astronomico di Trieste, Italy
[11] Department of Physics, University of Bristol, U.K.
[12] Institut de Ciències de l'Espai (CSIC), Barcelona, Spain
[13] Instituto Polictécnico Nacional, México D.F., México
[14] Laboratoire AIM Saclay, CEA/IRFU, CNRS/INSU, Université Paris Diderot, France
[15] Instituto de Física de Cantabria, CSIC-Univ. de Cantabria, Santander, Spain
[16] School of Physics and Astronomy, University of Birmingham, U.K.
[17] University College, Belfield, Dublin 4, Ireland
[18] INAF, Osservatorio Astronomico di Padova, Italy

Abstract

Aimed at understanding the evolution of galaxies in clusters, the GLACE survey is mapping a set of optical lines ([OII]3727, [OIII]5007, Hβ and Hα/[NII] when possible) in several galaxy clusters at $z \sim 0.40$, 0.63 and 0.86, using the Tuneable Filters (TF) of the OSIRIS instrument [7] at the 10.4 m GTC telescope. This study will address key questions about the physical processes acting upon the infalling galaxies during the course of hierarchical growth of clusters. GLACE is already ongoing: we present some preliminary results on our observations of the galaxy cluster Cl0024+1654 at $z = 0.395$; GLACE@0.86 has been approved as ESO/GTC large project to be started in 2011.

1 Introduction

The cores of nearby clusters are dominated by red early-type galaxies, suggesting a long period of passive evolution [5]. At higher redshifts, however, significant evolution in galaxy properties is well-known through the Butcher-Oemler (BO) effect [6]: the increase in the fraction of blue galaxies in clusters at $z > 0.2$. An equivalent increase in obscured star formation (SF) activity has also been seen in mid-IR surveys of distant clusters [8, 11] and equally an increasing population of AGN, have been found in more distant clusters. Even focusing on a single epoch, aspects of this same evolutionary trend have been discovered in the outer parts of clusters where significant changes in galaxy properties can be clearly identified such as gradients in typical colour or spectral properties with clustercentric distance [3, 22] and in the morphology-density relation [10]. In a hierarchical model of structure formation, galaxies merge into larger and larger systems as time progresses. It is quite likely that this accretion process is responsible for a transformation of the properties of cluster galaxies both as a function of redshift and as a function of environment [4, 16]. The central physical processes causing these evolutionary and environmental changes remains elusive [27]. Possible processes that have been proposed include: (i) Galaxy-ICM interactions: ram-pressure stripping, thermal evaporation of the ISM, turbulent and viscous stripping, pressure-triggered SF. When a slow decrease of the SF is produced, these mechanisms are collectively labelled as starvation. (ii) Galaxy-cluster gravitational potential interactions: tidal compression, tidal truncation. (iii) Galaxy-galaxy interactions: mergers (low-speed interactions), harassment (high-speed interactions). Nevertheless, we do not yet understand whether the correlations of star-formation histories and large-scale structure are due to the advanced evolution in overdense regions, or to a direct physical effect on the star formation capability of galaxies in dense environments [26]. This distinction can be made reliably if one has an accurate measurement of star formation rate (or history), for galaxies spanning a range of stellar mass and redshift, in different environments. The physical processes proposed above act on the star-forming (SF) and AGN population within the clusters. Although useful, broad-band photometric surveys are too crude to reliably assign membership or dynamics to individual

galaxies, or to conclusively show that they were SF. Narrow-band imaging surveys are much more productive than spectroscopic ones as a method to identify *all* the emission line galaxies (ELG) in a cluster. Nevertheless, "classical" narrow-band imaging suffers from ambiguity about the true fluxes of detected sources and does not provide dynamical information about the population.

2 The GLACE project: objectives and description

The GaLAxy Cluster Evolution survey (GLACE) is an innovative survey of ELG and AGN in a well-studied and well-defined sample of clusters in three narrow redshift windows, chosen to be relatively free of strong sky emission lines. This programme is undertaking panoramic census of the star formation and AGN activity within nine clusters at $z \sim 0.40$, 0.63 and 0.86, mapping a set of important lines: Hα (only at $z \sim 0.4$), Hβ, [OII]3727 and [OIII]5007; these maps of ELG are compared with the structures of these systems (as traced by galaxies, gas and dark matter) to address several crucial issues:

(1) Star formation in clusters: we will determine how the star formation properties of galaxies relate to their position in the large scale structure. This will provide a key diagnostic to test between different models for the environmental influence on galaxy evolution. Each mechanism is most effective in a different environment (generally depending on the cluster-centric distance, e.g. [27]), leaving a footprint in the data. We are mapping the extinction-corrected star formation through Hα and [OII], over a large and representative region in a statistically useful sample of clusters. The survey has been designed to reach SFR $\sim$2 $M_\odot$/yr (i.e. below that of the Milky Way) with 1 magnitude of extinction at Hα[1]. Our first results (see Section 3) indicate a good agreement with the requirement. Another important question that can be addressed is related with the kind of galaxies (type/mass) forming stars within clusters. The study of the morphology of confirmed ELGs allows investigating the connection between the truncation of star formation and the morphological transformation of infalling galaxies (e.g. [24]). In addition, by determining the total integrated star formation rates, we can construct a star-formation history for galaxies in clusters, as has been done in the field (e.g. [18]).

(2) The role of AGNs: whether the fraction of AGN is environment-dependent or not is a matter of debate: while some results [19] point towards a lack of depency of the AGN fraction with the local galaxy density, other authors [13] conclude that high-luminosity AGN do avoid high-density regions. Such a lack of AGN in clusters, as compared to the field, may be related to the evolution of galaxies as they enter the cluster environment. On the other hand, claims for an enhanced fraction of AGN in groups (e.g. [25]) point at AGN-stimulating processes such as galaxy–galaxy interactions or mergers that are particularly effective in the low-velocity dispersion and (relatively) high-density environments typical of groups (and filaments). A complete census of the AGN population in clusters at different redshifts, and in cluster regions characterized by different mean densities and velocity dispersions, can help us to constrain the physics behind the onset of the AGN activity in galaxies. Our survey is

[1] $f_{\mathrm{H}\alpha} = 1.89 \times 10^{-16}\,\mathrm{erg\,s^{-1}}$ at $z = 0.4$ using standard SFR–luminosity conversion factors [14].

sensitive to the AGN population within clusters, discriminated from pure star formation by means of standard diagnostics (e.g. BPT diagrams).

(3) The study of the distribution of galaxy metallicities with cluster radii is another potentially powerful mean to investigate evolution within clusters. As galaxies fall into clusters and travel toward the cluster center along their radial orbits, they interact with the intra-cluster medium (ICM) and other cluster galaxies, thus getting progressively stripped of their gas reservoir. This process is expected to influence their metal abundances and possibly generate a metallicity gradient across a cluster. Not much is yet known on the metallicities of emission-line galaxies in clusters and how it varies with cluster-centric distances. GLACE will allow to derive extinction-corrected metallicities using N2 [9], R23 [21], and O3N2 [2], where N2 and O3N2 will be used to break the R23 degeneracy and to assess possible differences between N and O abundances vs. metallicity.

The survey can address many other interesting topics: for instance the cluster accretion history can be traced by studying the census of ELGs at different cluster-centric distances. In addition, the survey will provide an accurate assessment of cluster membership, without the need of a spectroscopic follow-up.

Regarding the technical implementation, the GLACE survey applies the technique of TF tomography: for each line, a set of images are taken through the OSIRIS TF, each image tuned at a different wavelength (equally spaced), so that a rest frame velocity range of several thousands km s^{-1} (6500 km s^{-1} for our first target) centred at the mean cluster redshift is scanned for the full TF field of view of 8 arcmin in diameter. Additional images are taken to compensate for the blueshift of the wavelength from centre to the edge of the field of view. Finally, for each pointing and wavelength tuned, three dithered exposures allow correcting for etalon diametric ghosts, using combining sigma clipping algorithms.

The TF FWHM and sampling (i.e. the wavelength interval between consecutive exposures at Hα are of 1.2 and 0.6 nm, respectively, to allow deblending Hα from [NII]λ6584. with an accuracy better than 3%. For the rest of the lines, the largest available TF FWHM, 2.0 nm is applied, with sampling interval of 1.0 nm. These parameters allow a continuum subtraction accuracy better than 2% and a photometric accuracy better than 6%. The same pointing positions are observed at every emission line. We have required to cover $\simeq 2$ virial radii (some 4 Mpc) within the targeted clusters. This determines the number of OSIRIS pointings (2 at 0.4 and 0.63, 1 at 0.85).

3 Initial results

The first target chosen for the GLACE survey is the rich cluster Cl0024+1654 at $z = 0.395$; this object has been comprehensively studied; public catalogues[2] include photometric data for 73318 objects detected and extracted in the HST WFPC2 sparse mosaic covering 0.5×0.5 degrees [27] and in the ground-based CFHT CFH12k $BVRI$ and Palomar WIRC JK_s imaging. Visually determined morphological types are given for all objects brighter than $I = 22.5$. In addition, thousands of photometric and spectroscopic redshift estimates are available.

[2] http://www.astro.caltech.edu/∼smm/clusters/

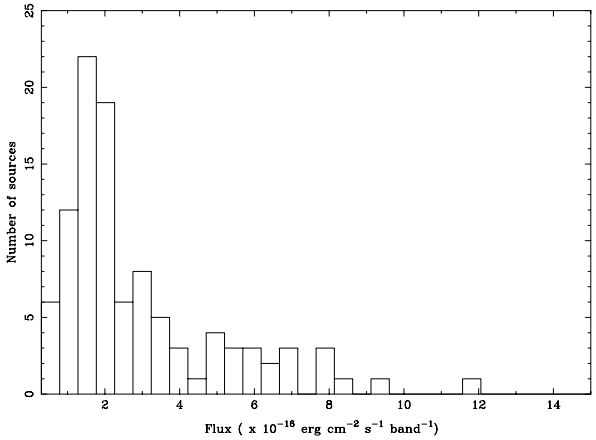

Figure 1: Flux histogram of the sub-sample of ELGs (103 sources). The fluxes represented here correspond to the maxima of the pseudo-spectra (i.e. line + continuum fluxes integrated within a single passband of 6Å FWHM).

The catalogue of spectroscopically confirmed objects within the field (including foreground, cluster and background sources) comprises 1632 sources (see [20] and references therein). A narrow-band Subaru Hα (plus $BVRI$ broadband) survey has been carried out [17], although this has an unknown selection function due to the narrow-band filter transmission, as well as lacking the velocity resolution and ability to deconvolve [NII] contributions of our OSIRIS observations.

So far, two observing campaigns (GTC semesters 09B and 10A), allocating a total of 18 hours have been completed. The red TF has been used to observe the [OIII]5007, Hβ and Hα/[NII] lines[3]. Here we present the first results on the processing of the Hα/[NII] complex (5.15 hours of on-source integration time, covering the 9047–9341 Å range in 50 scan steps). Data reduction was performed using a version of the TFRED package [12] modified for OSIRIS by A. Bongiovanni and private IDL scripts. Details of the processing are given in [23].

From our Hα/[NII] maps we have obtained a raw catalog of 1076 sources. In a first analysis, we have extracted 103 very robust (i.e. high S/N) emission line galaxies (ELG; comprise both star-forming galaxies and AGN). The completeness limit of the ELG sample (Fig. 1) is $\sim 1.5 \times 10^{-16}\,\mathrm{erg\,s^{-1}\,cm^{-2}\,band^{-1}}$ (line + continuum), i.e. very likely well within the GLACE requirements.

We have cross-matched our ELG catalogue with the public photometric and spectroscopic catalogues described above (see also [20]) by means of the Starlink TOPCAT tool using a search radius of 1.5 arcsec, finding 96 matches (93% of the sample). From these, a

[3]The [OII]3727 line will be observed when the blue TF and corresponding order sorting filters become available

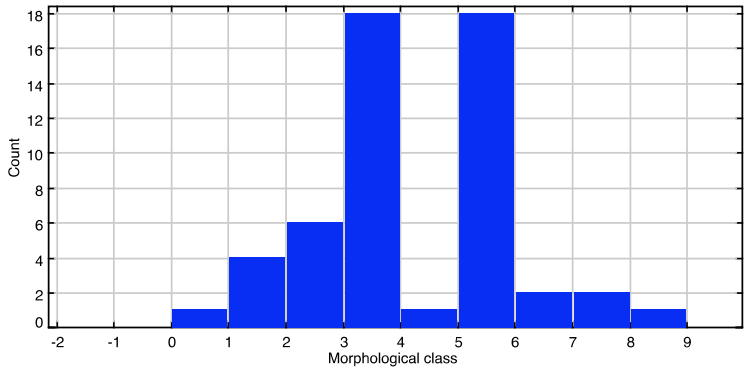

Figure 2: Morphological classification of the robust ELG detections, according to [1]: $-2 =$ star, $-1 =$ compact, $0 =$ E, $1 =$ E/S0, $2 =$ S0, $3 =$ Sab, $4 =$ S, $5 =$ Scdm, $6 =$ Irr, $7 =$ peculiar, $8 =$ merger, $9 =$ defect.

morphological type was available for 53 objects (see Fig. 2). As expected, most of the ELGs are spiral galaxies (37), with a minor fraction of irregular, peculiar or mergers (5 objects). However, a significant fraction of the ELGs (10 sources) are early-type galaxies.

Redshift estimates were available for 90 of our ELGs. From these, a vast majority (83) have a redshift close to that of the cluster. There was a remarkably good agreement between the redshift estimates derived from the position of the Hα line within our pseudo-spectra (see some examples in Fig. 3) and that derived from spectroscopic measurements. Work in progress includes a precise deblending of the Hα and [NII] lines and an accurate determination of the line wavelengths (the maxima in the pseudo-spectra plotted correspond to the central wavelength of the scan including the actual line maximum; this has therefore an uncertainty of ± 3 Å). This information will in turn allow us to establish cluster membership, galaxy dynamics, star formation rate and/or AGN nature of the emission.

The spatial distribution of the ELG sample is depicted in Fig. 4 and maps the presence of two components: (i) a structure assembling onto the cluster core from the NW with an orientation almost in the plane of the sky. This structure has been already reported by other authors [20, 28, 15]. (ii) An infalling group at high velocity nearly along the line of sight to the cluster centre [20].

Acknowledgments

This work was supported by the Spanish Plan Nacional de Astronomía y Astrofísica under grant AYA2008–06311–C02–01. We acknowledge support from the Faculty of the European Space Astronomy Centre (ESAC). Based on observations made with the Gran Telescopio Canarias (GTC), installed in the Spanish Observatorio del Roque de los Muchachos of the Instituto de Astrofísica de Canarias, in the island of La Palma.

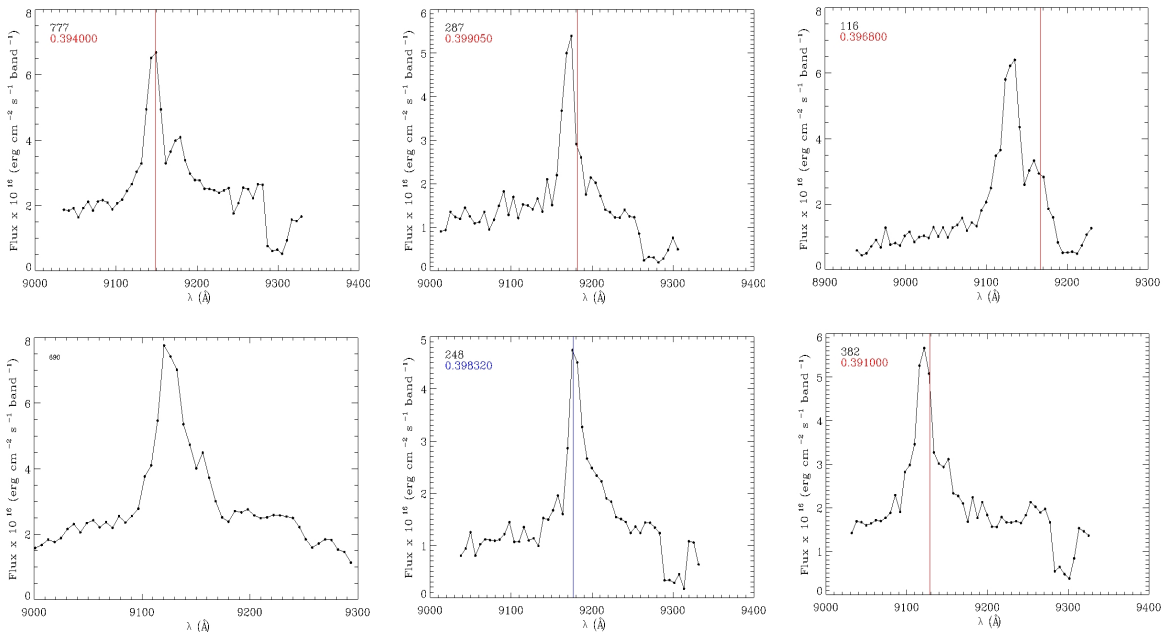

Figure 3: Examples of pseudo-spectra built from the Hα scan (50 steps). Generally one of the [NII] doublet components is clearly resolved. When available, redshifts from the public catalogue have been included (blue–spectroscopic redshift from Keck/DEIMOS, red–spectroscopic redshift from other sources).

References

[1] Abraham, R., et al. 1996, ApJS, 107, 1

[2] Alloin, D., et al. 1979, A&A, 78, 200

[3] Balogh, M., et al. 1999, ApJ, 527, 54

[4] Balogh, M., et al. 2000, ApJ, 540, 113

[5] Bower, R. G., et al. 1998, MNRAS, 299, 1193

[6] Butcher, H., & Oemler, A. 1984, ApJ, 285, 426

[7] Cepa, J., et al. 2005, RevMexAA, 24, 1

[8] Coia, D., et al. 2005, A&A, 430, 59

[9] Denicoló, G., et al. 2002, MNRAS, 330, 69

[10] Dressler, A., et al. 1997, ApJ, 490, 577

[11] Geach, J., et al. 2006, ApJ, 649, 661

[12] Jones, D. H., et al. 2002, MNRAS 329, 759

[13] Kauffman, G., et al. 2004, MNRAS, 353, 713

[14] Kennicutt, R. C. 1998, ARA&A, 36, 189

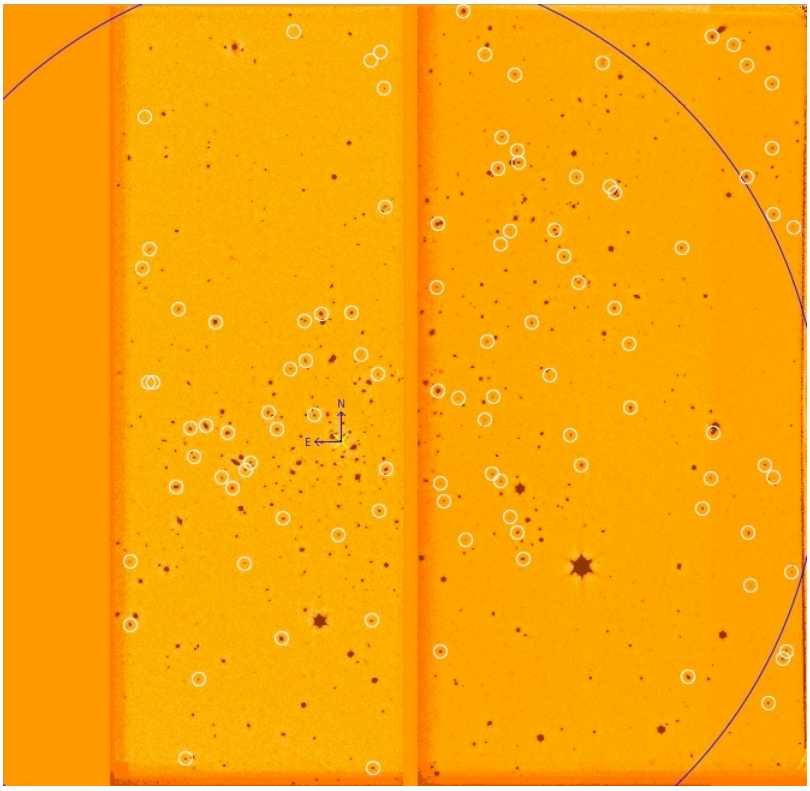

Figure 4: Deep cluster image obtained by adding up all the scan steps. The light circles enclose robust ELG detections. The cross symbox ($\times$) marks the cluster centre. The large blue circle corresponds to $r_{\rm vir}$.

[15] Kneib, J.-P., et al. 2003, ApJ, 598, 804
[16] Kodama, T., & Bower, R. 2001, MNRAS, 321, 18
[17] Kodama, T., et al. 2004, MNRAS, 354, 1103
[18] Madau, P., et al. 1998, ApJ, 498, 106
[19] Miller, C. J., et al. 2003, ApJ, 597, 142
[20] Moran, S., et al. 2007, ApJ, 671, 1503
[21] Pagel, B. E. J., et al. 1979, MNRAS, 189, 95
[22] Pimbblet, K.A., et al. 2001, MNRAS, 327, 588
[23] Pintos-Castro, I., et al. 2010, these proceedings
[24] Poggianti, B., et al. 1999, ApJ, 518, 576
[25] Popesso, P., & Biviano, A. 2006, A&A, 460, L23
[26] Popesso, P., et al. 2007, A&A, 461, 411
[27] Treu, T., et al. 2003, ApJ, 591, 53
[28] Zhang, Y.-Y., et al. 2005, A&A, 429, 8